SLAC-PUB-13417
BABAR-PROC-08/129
October 2008

$\alpha(\phi_2)$ from a time-dependent analysis of $B^0 \to (\rho\pi)^0$ Dalitz-plot

Gagan B. Mohanty
From the BABAR Collaboration
Department of Physics, University of Warwick, Coventry CV4 7AL, UK

Abstract

We present results of time-dependent Dalitz plot analyses of $B^0 \to (\rho\pi)^0$ and the corresponding constraints on the angle α or ϕ_2 of the CKM unitarity triangle from the B factories.

Presented at the Fifth International Workshop on the CKM Unitarity Triangle,
Rome, Italy, 9-13 September 2008.

Stanford Linear Accelerator Center, Stanford University, Stanford, CA 94309

Work supported in part by the UK Science and Technology Facilities Council and the US Department of Energy under contract DE-AC02-76SF00515.

1 Introduction

A precise measurement of the angle α (or ϕ_2) in the unitarity triangle is important for the complete test of the Cabibbo-Kobayashi-Maskawa (CKM) paradigm [1] that describes quark mixing and charge-parity (*CP*) violation in the Standard Model. Synder and Quinn have proposed a theoretically clean method [2] to extract this angle in the decays $B^0 \to (\rho\pi)^0$ [3] by explicitly taking into account the variation of the strong phase of interfering ρ resonances in the three-pion Dalitz plot. In this report, we summarize the experimental constraints on the CKM angle α from a time-dependent Dalitz plot analysis (TDPA) of $B^0 \to (\rho\pi)^0$, studied using e^+e^- collision data collected near the $\Upsilon(4S)$ resonance by the two B-factory experiments: *BABAR* at SLAC [4] and Belle at KEK [5]. Details on the measurements of α from the decays $B^0 \to \pi^+\pi^-$ and $\rho^+\rho^-$ can be found in Ref. [6].

2 TDPA Formulation

The decay of a neutral B meson into the three-pion final state, through an intermediate ρ meson, occurs via two topologies: the $b \to u$ CKM-suppressed tree transition and the $b \to d$ penguin (loop) diagram. The *CP* violation parameter λ, defined by $\lambda = \frac{q}{p}\frac{\overline{A}}{A}$, where the ratio $\frac{q}{p}$ is linked to *CP* violation in mixing of neutral B mesons and A ($\overline{A}$) is the amplitude of the B^0 ($\overline{B}^0$) decays to $(\rho\pi)^0$, can be expressed in terms of the angle α as

$$\lambda = \mathrm{e}^{2i\alpha}\,\frac{1 - \left|\frac{V_{td}^* V_{tb}}{V_{ud}^* V_{ub}}\right| (P/T)\mathrm{e}^{-i\alpha}}{1 - \left|\frac{V_{td}^* V_{tb}}{V_{ud}^* V_{ub}}\right| (P/T)\mathrm{e}^{i\alpha}}. \tag{1}$$

Here T and P are complex amplitudes dominated by the tree and the penguin diagrams, respectively, and $V_{qq'}$ denotes the CKM matrix element. Experimentally, one measures the time-dependent decay rate

$$f^{\rho\pi}_{Q_{tag}}(\Delta t) = (1 \pm A_{CP})\frac{\mathrm{e}^{-|\Delta t|/\tau}}{4\tau}[1 - Q_{tag}(C \pm \Delta C)\cos(\Delta m_d \Delta t) + Q_{tag}(S \pm \Delta S)\sin(\Delta m_d \Delta t)] \tag{2}$$

where Δt is the proper decay time difference between the B meson decaying to $(\rho\pi)^0$ and the other B in the event, denoted B_{tag}. Δm_d is the B^0–$\overline{B}^0$ mixing frequency and τ is the neutral B lifetime. Q_{tag} is set $+1(-1)$ if the B_{tag} is a $B^0(\overline{B}^0)$. The time-dependent *CP* asymmetries C and S are related to the parameter λ by

$$C = \frac{1 - |\lambda|^2}{1 + |\lambda|^2}, \qquad S = \frac{2\,\mathrm{Im}(\lambda)}{1 + |\lambda|^2}. \tag{3}$$

A_{CP} is the time- and flavor-integrated *CP* violation parameter, measuring the asymmetry between the $\rho^+\pi^-$ and $\rho^-\pi^+$ final states, whereas ΔC and ΔS, which arise from the fact that two production modes of the ρ are possible, are dilution terms and have no *CP* content.

The ingenuity of the Snyder-Quinn approach came from the realization that $(\rho\pi)^0$ is an intermediate state which further decays to a three-pseudoscalar final state of $\pi^+\pi^-\pi^0$

and hence one can extend the time-dependent decay rate, presented in Eq. (2), to explicitly include the Dalitz-plot dependence. We can rewrite the expression as

$$f_{Q_{tag}}^{\rho\pi}(\Delta t) \propto \left[1 - Q_{tag}\frac{|A_{3\pi}|^2 - |\overline{A}_{3\pi}|^2}{|A_{3\pi}|^2 + |\overline{A}_{3\pi}|^2}\cos(\Delta m_d \Delta t) + Q_{tag}\frac{2\,\mathrm{Im}(\frac{q}{p}A_{3\pi}^*\overline{A}_{3\pi})}{|A_{3\pi}|^2 + |\overline{A}_{3\pi}|^2}\sin(\Delta m_d \Delta t)\right], \tag{4}$$

where

$$A_{3\pi} \equiv A_{3\pi}(m^2_{\pi^+\pi^0}, m^2_{\pi^-\pi^0}) = \sum_{\kappa\in\{+,-,0\}} f_\kappa(m^2_{\pi^+\pi^0}, m^2_{\pi^-\pi^0})A_\kappa\,. \tag{5}$$

f_κ is the term that absorbs all the dependence on Dalitz-plot variables $m^2_{\pi^+\pi^0}$ and $m^2_{\pi^-\pi^0}$, and A_κ is the complex amplitude whose magnitude and phase determine the relative fraction and interference pattern of the intermediate resonance. The index κ runs over three possible charge states of the ρ meson.

Substituting Eq. (5) and a similar expression for $\overline{A}_{3\pi}$, coefficients of the sine and cosine terms in Eq. (4) can be expressed in terms of 27 form factor bilinears (U, I) [7]:

$$|A_{3\pi}|^2 \pm |\overline{A}_{3\pi}|^2 = \sum_\kappa |f_\kappa|^2 U_\kappa^\pm + 2\sum_{\kappa<\sigma}\left(\mathrm{Re}[f_\kappa f_\sigma^*]U_{\kappa\sigma}^{\pm,\mathrm{Re}} - \mathrm{Im}[f_\kappa f_\sigma^*]U_{\kappa\sigma}^{\pm,\mathrm{Im}}\right),$$
$$\mathrm{Im}\left(\frac{q}{p}A_{3\pi}^*\overline{A}_{3\pi}\right) = \sum_\kappa |f_\kappa|^2 I_\kappa + \sum_{\kappa<\sigma}\left(\mathrm{Re}[f_\kappa f_\sigma^*]I_{\kappa\sigma}^{\mathrm{Im}} + \mathrm{Im}[f_\kappa f_\sigma^*]I_{\kappa\sigma}^{\mathrm{Re}}\right)\,. \tag{6}$$

These real-valued coefficients are the observables that are determined from the fit. Each of them is related in a unique way to physically more intuitive quantities, such as tree-level and penguin-transition amplitudes, the CKM angle α, or the *CP* violation and dilution parameters of the quasi-two-body intermediate resonances.

3 Experimental Techniques

$B^0 \to (\rho\pi)^0 \to \pi^+\pi^-\pi^0$ decay events are reconstructed by combining two charged pions with a neutral pion, which is in turn formed out of two electromagnetic clusters consistent with photons. Dedicated subdetectors (a Cherenkov detector based on total internal reflection in case of *BABAR*, and Aerogel Cherenkov threshold detector and time-of-flight counter for Belle) are employed to separate charged pions from kaon track candidates.

The continuum light-quark pair production, $e^+e^- \to q\overline{q}\,(q = u, d, s, c)$, forms the most dominant background component. It is suppressed by exploiting the difference in event topology – B mesons are produced almost at rest resulting in a spherical event, while the light-quark pairs tend to have a jetlike shape owing to the large available kinetic energy. *BABAR* combines the topological information into an artificial neural network and later uses its output as one of the input variables in the multidimensional likelihood fit. Belle, in contrast, forms a likelihood ratio and imposes a requirement on it to reject continuum events.

The signal yields and the form factor bilinears are determined in unbinned maximum-likelihood fits to Δt, Dalitz-plot variables and kinematic quantities that make use of precise beam-energy information and energy-momentum conservation. The kinematic variables are the difference ΔE between the energy of the reconstructed B candidate and the beam energy ($E_{\rm beam}$), and the beam-energy substituted mass $m_{\rm ES} \equiv \sqrt{E^2_{\rm beam} - \mathbf{p}^2_B}$, where $\mathbf{p}_B$ is the momentum of the B candidate (here the B candidate's energy and momentum are calculated in the $\Upsilon(4S)$ rest frame). Signal events are expected to peak around the nominal B mass [8] for $m_{\rm ES}$ and near zero for ΔE.

4 Results

With datasets containing 375×10^6 and 449×10^6 $B\overline{B}$ decays, *BABAR* [10] and Belle [11] report inclusive signal yields of 2067 ± 86 and 971 ± 42 events, respectively. There is an excellent agreement between the two experiments for the measured form factor bilinears ($\chi^2 = 19.0$ for 26 degrees of freedom [9]). As described earlier, these bilinears can be translated into a number of physically more intuitive parameters, which are presented in Table 1.

Table 1: Summary of the quasi-two-body CP observables in $B^0 \to (\rho\pi)^0$ decays. Quoted uncertainties are statistical and systematic, respectively.

Expt	C	S	A_{CP}
BABAR	$0.15 \pm 0.09 \pm 0.05$	$-0.03 \pm 0.11 \pm 0.04$	$-0.14 \pm 0.05 \pm 0.02$
Belle	$-0.13 \pm 0.09 \pm 0.05$	$0.06 \pm 0.13 \pm 0.05$	$-0.12 \pm 0.05 \pm 0.04$
	ΔC	ΔS	
BABAR	$0.39 \pm 0.09 \pm 0.09$	$-0.01 \pm 0.14 \pm 0.06$	
Belle	$0.36 \pm 0.10 \pm 0.05$	$-0.08 \pm 0.13 \pm 0.05$	

From the measured bilinears, *BABAR* extracts a confidence level (C.L.) interpretation for the angle α, and constrains $\alpha = \left(87^{+45}_{-13}\right)^\circ$ at 68 % C.L.. *BABAR* has also measured the relative strong phase difference, δ_{+-}, between the amplitudes of the decays $B^0 \to \rho^+\pi^-$ and $B^0 \to \rho^-\pi^+$ to be $(37 \pm 37)^\circ$. Belle has performed a similar analysis. In addition, it has also included information from all the SU(2) components of $B \to \rho\pi$, which can be used to constrain $\alpha \equiv \phi_2$ via the isospin relation. The isospin analysis uses as input the branching fractions and CP violation asymmetries of five possible $\rho\pi$ decay modes [9]; namely $\rho^\pm\pi^\mp$, $\rho^0\pi^0$, $\rho^+\pi^0$ and $\rho^0\pi^+$. With all this information put together, Belle obtains the constraint $68^\circ < \phi_2 < 95^\circ$ at 68 % C.L., for the solution consistent with the Standard Model. Figure 1 shows the C.L. function vs. angle α for the two experiments.

5 Conclusions

Both of the B-factory experiments have implemented the Synder-Quinn approach to extract the CKM angle α without any trigonometric ambiguity, thanks to the Dalitz-plot technique. The current precision is heavily limited due to statistics – almost no constraint is obtained

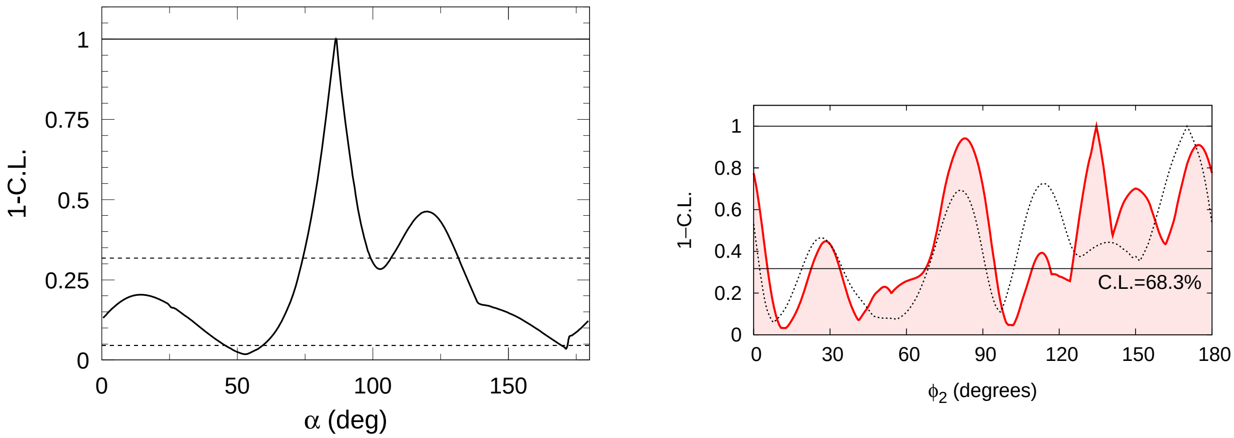

Figure 1: C.L. as a function of the angle α (or ϕ_2) for *BABAR* (left) and Belle (right). The *BABAR* result shows the additional constraint at 2σ indicated by the dashed line near $1 - \text{C.L.} = 0.05$, while for Belle the result also includes the isospin analysis (solid red curve).

at the 2σ level. Clearly, it would be imperative for the B factories to update this important analysis with a larger dataset. (To that end, they have already accumulated 70% more data between them.) The upcoming LHCb experiment at CERN is projected to give a competitive limit [12], albeit with limited leverage on the neutral cluster reconstruction. The proposed super flavor factory [13] would really pin down the angle α using this approach in conjunction with results from the isospin analyses of $B^0 \to \pi^+\pi^-$ and $\rho^+\rho^-$.

References

[1] N. Cabibbo, Phys. Rev. Lett. **10**, 531 (1963); M. Kobayashi and T. Maskawa, Prog. Theor. Phys. **49**, 652 (1973).

[2] H.R. Quinn and A.E. Synder, Phys. Rev. D **48**, 2139 (1993).

[3] Charge conjugates are included implicitly throughout.

[4] B. Aubert *et al.* [*BABAR* Collaboration], Nucl. Instr. Methods Phys. Res., Sect. A **479**, 1 (2002).

[5] A. Abashian *et al.* [Belle Collaboration], Nucl. Instr. Methods Phys. Res., Sect. A **479**, 117 (2002).

[6] See talks by A.V. Telnov and A.J. Schwartz at this conference.

[7] H.R. Quinn and J.P. Silva, Phys. Rev. D **62**, 054002 (2000).

[8] C. Amsler *et al.* [Particle Data Group], Phys. Lett. B **667**, 1 (2008).

[9] E. Barberio *et al.* [Heavy Flavor Averaging Group], arXiv:0808.1297 [hep-ex] and online update at `http://www.slac.stanford.edu/xorg/hfag`.

[10] B. Aubert *et al.* [*BABAR* Collaboration], Phys. Rev. D **76**, 012004 (2007).

[11] A. Kusaka *et al.* [Belle Collaboration], Phys. Rev. Lett. **98**, 221602 (2007); Phys. Rev. D **77**, 072001 (2008).

[12] O. Deschamps *et al.*, LHCb-2007-046 (2007).

[13] M. Bona *et al.* [SuperB Conceptual Design Report], arXiv:0709.0451 [hep-ex]; A.G. Akeroyd *et al.* [SuperKEKB Physics Working Group], arXiv:hep-ex[0406071].